

Optimal seismic retrofitting of frame structures using hysteretic dampers

Y. Daniel, & O. Lavan

Technion- Israel Institute of Technology, Israel

R. Levy

Ben Gurion University, Israel



SUMMARY:

This paper presents a methodology for the optimal seismic performance-based design of frames using hysteretic dampers as a means for passive control. The design methodology is of the analysis/redesign type. It attains the stiffness of the individual braces and their strength. This procedure resulted in a fully stressed design, i.e. a device was added only where the performance equaled the allowable value. In this paper, a formal gradient-based solution to the same optimization problem is offered. The connection between optimal solution obtained by this methodology and the solution obtained using the simple analysis/redesign algorithm is then studied and discussed.

Keywords: Seismic Design, Friction dampers, Performance-Based Design, Fully-Stressed Design, Optimization.

1. INTRODUCTION

Seismic design of structures is a very intriguing and important issue in the field of structural engineering. Severe earthquakes are not a very common event and are random in nature, making them hard to predict and design for. However, once they occur, life threatening situations and major structural destruction are likely to happen. Structural performance is highly related to damage states within the structure. Some response measures often associated with damage are drifts and energy dissipation, and structural performance can be efficiently achieved by controlling these parameters.

One way of controlling responses and enhancing seismic performance within an existing structure is by adding external control systems. Clearly, the design of structures with added control systems should be cost-effective as well as practical and intuitive for the use of practicing engineers. Passive friction dampers that dissipate energy through Coulomb friction forces created between two solids during slippage are considered in this section. The hysteretic model of friction dampers is a stick-slip one, with the slip displacement being smaller than the yielding displacement of the brace, to ensure the device slips. The hysteretic curves of these dampers are usually rectangular, show large dissipation abilities, and exhibit nearly no fade over a large number of cycles (Symans *et al.*, 2008; Soong and Dargush, 1997). They are also relatively simple to model (and are therefore more familiar to the practicing engineer) and are commonly used worldwide. A similar hysteretic behaviour can be attained by using metallic yielding devices. In this case, the energy is dissipated through yielding of metal components. Therefore, the optimization problem presented herein as well as its solution can generally be used with any type of hysteretic damping device.

Since hysteretic devices have been extensively studied over the last few decades, several methodologies for the allocation of such dampers exist. Among the non-optimal design methodologies are methodologies which predetermine the damping distribution. These include the methodologies presented by Cherry and Filiatrault (1993), Inoue and Kuwahara (1998), Levy *et al.* (2001, 2005), Choi and Kim (2006), Lee *et al.* (2008), Benavent-Climent (2011). Other methodologies, such as Lopez Garcia (2001), Liu *et al.* (2005), Xu and Teng (2002), Yang *et al.* (2002), Moreschi and Singh

(2003), Wongprasert and Symans (2004), Dargush and Sant (2005), Ok *et al.* (2008), Apostolakis and Dargush (2010), Farhat *et al.* (2009) Lavan and Dargush (2009) and Daniel *et al.* (2010), are optimal, or close to optimal. Although these methods are considered optimal, a great portion of the end result depends on the performance measure and objective function chosen. Often, these optimal solutions are very computationally expensive or are otherwise not very practical to apply. This paper presents a design methodology that is both cost-efficient, being optimal or near-optimal and practical to apply. Moreover, it may be regarded as optimal since a comparison of its designs to those attained by a formal optimization shows close matchup.

2. PROBLEM FORMULATION

2.1. Equations of motion

The differential equations of motion for a yielding MDOF structure with added hysteretic damping devices undergoing seismic loading are formulated as:

$$\begin{aligned} \mathbf{M}\ddot{\mathbf{x}}(t) + \mathbf{C}\dot{\mathbf{x}}(t) + \mathbf{K}_a\mathbf{x}(t) + \mathbf{f}_h(\mathbf{x}(t), \dot{\mathbf{x}}(t)) + \mathbf{f}_{h_0}(\mathbf{x}(t), \dot{\mathbf{x}}(t)) &= -\mathbf{M}\mathbf{e}a_g(t); & \mathbf{x}(0) = \mathbf{0}, \dot{\mathbf{x}}(0) = \mathbf{0} \\ \dot{\mathbf{f}}_h(t) &= f(\dot{\mathbf{x}}(t), \mathbf{f}_h(t)); & \mathbf{f}_h(0) = \mathbf{0} \\ \dot{\mathbf{f}}_{h_0}(t) &= f(\dot{\mathbf{x}}(t), \mathbf{f}_{h_0}(t), \mathbf{k}_0); & \mathbf{f}_{h_0}(0) = \mathbf{0} \end{aligned} \quad (2.1)$$

where \mathbf{M} and \mathbf{C} are the mass and inherent damping matrices of the bare structure in inter-story drift DOFs, \mathbf{K}_a represents the stiffness matrix (in drift DOFs) of the structure after yielding, $a_g(t)$ is the ground motion's acceleration function, \mathbf{e} is the excitation direction matrix with values of zero and one, $\ddot{\mathbf{x}}(t)$, $\dot{\mathbf{x}}(t)$ and $\mathbf{x}(t)$ are the relative inter-story acceleration, velocity and displacement vectors between the DOFs and the ground, $\mathbf{f}_h(\mathbf{x}(t), \dot{\mathbf{x}}(t))$ and $\mathbf{f}_{h_0}(\mathbf{x}(t), \dot{\mathbf{x}}(t))$ are the hysteretic force vector of the yielding structure and dampers, accordingly, in local drift coordinates with zero secondary slope. \mathbf{k}_0 represents the vector of added brace stiffness. This representation assumes a bi-linear representation (e.g. Sivaselvan and Reinhorn, 2000) of the hysteretic behavior of the yielding structure and damper, with the friction damper having a zero-stiffness after slipping occurs. An example for a differential form of the hysteretic force relationship is Ozdemir's rate-independent model (Ozdemir, 1976).

2.2. Performance measures

Structural performance, in this case, is evaluated on the basis of damage. This is done using existing damage indices, or any other response found to portray structural damage due to seismic action. It seems that in the case of structures which stay within the elastic zone following a seismic incident, damage is strongly related to the maximal inter-story drift developed. Otherwise, it seems more appropriate to use an accumulated-natured performance measure, relating to both drifts and hysteretic energy. It should be emphasized that in the following optimization problem damage is limited on a local basis, i.e. in each story separately. Hence, the problem formulation, as well as the design procedure to be presented, are appropriate for both regular and irregular structures. Added friction dampers help reduce these performance measures, and the measure of cost and effectiveness of these devices is by the amount of added stiffness. The amount of added stiffness represents the cost of the retrofit, in addition to the fact that minimum added stiffness to the structure results in smaller added forces to the structure and smaller accelerations. In some cases, the installation of the device also has a fixed price which is independent of the stiffness of the device. As will be seen, the proposed methodology, indirectly, also reduces the number of added dampers, as those are allocated only where actually needed.

2.3. Optimization problem

The problem at hand is formulated as an optimization problem for which the objective function minimizes the total amount of added stiffness within the damping devices under constraints of

maximal performance measures. The optimization problem is thus formulated as:

$$\begin{aligned} \min_{\mathbf{k}_0} J &= \sum_{i=1}^{\text{No. of dampers}} \mathbf{k}_{0,i} = \mathbf{k}_0^T \cdot \mathbf{1} \\ \text{s.t.} \quad & pi_n \leq 1.0; \quad \mathbf{0} \leq \mathbf{k}_0 \leq \mathbf{k}_{0,\max} \end{aligned} \quad (2.2)$$

where \mathbf{k}_0 and $\mathbf{k}_{0,\max}$ are the vectors of added brace stiffness and maximal allowable added stiffness, and pi_n is a normalized inter-story performance index of interest.

3. PROPOSED SOLUTION SCHEMES

Two solution schemes are presented in this paper. The first is a solution scheme which is based on a simple analysis/redesign iterative process which leads to a "fully-stressed design" (FSD). This simple algorithm leads to solutions that are optimal as verified by a proposed second solution scheme, based on formal gradient-based optimization.

3.1. Fully stressed design and analysis/redesign algorithm

Designs that are based on fully stressed characteristics go back to the classical design of trusses under static loads, whereby the weight is minimized for a given allowable stress. For that problem it had been widely accepted that the optimal design yields a: *statically determinate fully stressed design, with members out of the design (i.e. with zero weight) having strains smaller than the allowable*. This result appeared in the literature as early as 1900 (Cilley, 1900). It was later shown (Levy, 1985) that this design is a Karush-Kuhn-Tucker point and therefore, an optimal design. Later on, it was shown that some dynamic optimal designs also possess "fully stressed" characteristics. Levy and Lavan (2006) considered the minimization of total added viscous damping to frame structures subjected to ground accelerations while constraining various inter-story responses. Their optimal solutions attained by formal optimization indicated that: *"At the optimum, damping is assigned to stories for which the local performance index has reached the allowable value. Stories with no assigned damping attain a local performance index which is lower or equal to the allowable."* That is, the optimal solutions attained "fully stressed design" characteristics. Based on past experience in similar problems and on the discussion in Lavan and Dargush (2009), where it was shown that the optimal buckling-restrained braces (BRB) allocation solution obtained using genetic algorithms (GA) is a FSD (or very close to that, since the problem was discrete), it is conjectured here that the optimal solution to the friction damper allocation and sizing problem in frame structures (the solution of Eqn. 2.2) possesses FSD characteristics, i.e.: *At the optimum, friction dampers are assigned to locations for which the inter-story performance index of interest has reached the allowable value under a given ensemble of ground motions*.

Solutions to optimization problems, which possess fully stressed characteristics, are efficiently achieved iteratively using a two-step algorithm in each iteration cycle. Such an analysis/redesign procedure will be utilized here to attain fully stressed designs where the stiffnesses and locations of the damping devices within frame structures are to be determined. The general recurrence formula used in this case is:

$$k_{0,i}^{(n+1)} = k_{0,i}^{(n)} \cdot \left(\frac{pi_i^{(n)}}{pi_{allowable}^i} \right)^P \quad (3.1)$$

where $k_{0,i}$ is the value of the design variable associated with location i , pi_i is the inter-story performance measure of interest at the location i , $pi_{allowable}^i$ is the allowable value for the performance measure, n - the iteration number and P - a convergence parameter.

3.2. Proposed analysis/redesign methodology

The first design methodology, which is based on an analysis/redesign iterative procedure to retrieve the solution to the optimization problem presented in Eqn. 2.2, is summarized in Table 3.1.

Table 3.1. Analysis/redesign optimization scheme flowchart

Step 1:	Perform time history analysis on the bare frame for all ground motion within the ensemble, evaluate the peripheral inter-story performance measures and check violation of the allowable performance measure. If the performance measure exceeds the allowable at any location, add friction dampers at the peripheral locations with a predetermined slip displacement and an arbitrary initial stiffness.
Step 2:	Perform time history analysis of the braced frame for all ground motions within the ensemble and re-evaluate the peripheral inter-story performance measures.
Step 3:	Using Eqn. 3.1, redesign each brace's stiffness according to the performance measure at that specific peripheral location.
Step 4:	Repeat steps 4 and 5 until convergence of all brace stiffnesses is reached.

3.3. Formal optimization scheme

The second design methodology uses gradient-based formal optimization tools to obtain the solution to the optimization problem presented in Eqn. 2.2. The actual optimization process was carried out using the MATLAB optimization toolbox, while supplying analytical expressions for the gradients of the objective function and constraints. There is a possibility, in these optimization algorithms to use gradients which are based on finite-differences. However, these require much computation effort which may be avoided when the gradients are provided.

3.3.1. Optimization algorithms

Not many optimization methods which are able to solve nonlinear constrained optimization problems (i.e., those whose objective function or constraints are nonlinearly dependent on the design parameter) exist. In the MATLAB Optimization Toolbox, two such gradient-based algorithms are available for use with the *fmincon* function. Those are the "Active Set" and "Interior Point" methods. Both these algorithms generally transform the original problem into a subproblem which is easier to solve, and use the solution to this subproblem to advance the solution towards the optimal solution.

3.3.2. Gradient computation

The gradients of the objective function and the constraints of the optimization problem introduced in Eqn. 2.2 are needed in order to formally solve the problem using gradient-based methods. The gradient of the objective function is computed in a straight-forward way and is $\nabla_{\mathbf{k}_0} J = \mathbf{1}$. As for the gradient of the constraints, these first have to be defined and formulated before their gradient can be derived. In the case of a yielding structure, taking into account the contribution of both maximal drifts and hysteretic energy dissipated (at the end of vibration) by yielding of the structure seems to agree with the approach to damage quantification. Thus, in this case the constraints ensure that at each location the drift is smaller than the allowable and the dissipated energy is smaller than the allowable. Here, average responses of an ensemble of ground motion are used (e.g. ASCE/SEI 41-06, 2007). In order to reduce computational efforts when evaluating the gradient, all performance measures can be combined into a single constraint. In the case where average values are used, the single constraint, p_i , represents the maximum between the maximal (of all locations) average (of all ground motions) normalized hysteretic energy and the maximal (of all locations) average (of all ground motions) normalized drift, and shall be smaller than one. This constraint can be written as:

$$pi = \max \left(\max_i \left(\frac{1}{n_{eq}} \sum_{n=1}^{n_{eq}} (\mathbf{E}_h(t_f))_n \right), \max_i \left(\frac{1}{n_{eq}} \sum_{n=1}^{n_{eq}} (\mathbf{d}_m)_n \right) \right) \leq 1.0 \quad (3.2)$$

where $\mathbf{E}_h(t_f)$ is a vector of the normalized hysteretic energy at the end of vibration obtained for a specific ground motion, \mathbf{d}_m is the vector of normalized maximal inter-story drifts obtained for a specific ground motion and n_{eq} is the number of ground motions considered. Or, equivalently, using a weighted sum (Lavan, 2006):

$$pi = \frac{\mathbf{1}^T \cdot \mathcal{D}^{q+1} \left(\frac{1}{n_{eq}} \sum_{n=1}^{n_{eq}} (\mathbf{E}_h(t_f))_n \right) \cdot \mathbf{1} + \mathbf{1}^T \cdot \mathcal{D}^{q+1} \left(\frac{1}{n_{eq}} \sum_{n=1}^{n_{eq}} \mathcal{D}^{\frac{1}{p}} (\mathbf{d}_{m,p}(t_f))_n \right) \cdot \mathbf{1}}{\mathbf{1}^T \cdot \mathcal{D}^q \left(\frac{1}{n_{eq}} \sum_{n=1}^{n_{eq}} (\mathbf{E}_h(t_f))_n \right) \cdot \mathbf{1} + \mathbf{1}^T \cdot \mathcal{D}^q \left(\frac{1}{n_{eq}} \sum_{n=1}^{n_{eq}} \mathcal{D}^{\frac{1}{p}} (\mathbf{d}_{m,p}(t_f))_n \right) \cdot \mathbf{1}} \leq 1 \quad (3.3)$$

where q is a large number, and the maximal inter-story drift is obtained using a p -norm (Lavan, 2006)

such that: $\mathbf{d}_m \approx \mathbf{d}_m(t_f) = \left(\frac{1}{t_f} \cdot \int_{t_0}^{t_f} (\mathcal{D}^{-1}(\mathbf{d}_{all}) \cdot \mathcal{D}(\mathbf{x}(t)))^p dt \right)^{\frac{1}{p}} \cdot \mathbf{1} = (\mathcal{D}(\mathbf{d}_{m,p}(t_f)))^{\frac{1}{p}} \cdot \mathbf{1}$, where p is a large positive even number. The gradient of this constraint was analytically derived and is:

$$\nabla_{\mathbf{k}_0} pi(\mathbf{k}_0) = \int_{t_0}^{t_f} \left\{ \left[\frac{\partial \mathbf{f}(\mathbf{v}(t), \mathbf{f}_{h0}(t), \mathbf{k}_0)}{\partial \mathbf{k}_0} \right]^T \cdot \boldsymbol{\lambda}_{th0}(t) \right\}_1 + \dots + \left\{ \left[\frac{\partial \mathbf{f}(\mathbf{v}(t), \mathbf{f}_{h0}(t), \mathbf{k}_0)}{\partial \mathbf{k}_0} \right]^T \cdot \boldsymbol{\lambda}_{th0}(t) \right\}_{n_{eq}} dt \quad (3.4)$$

$\boldsymbol{\lambda}_{th0}$ is a vector of Lagrange multipliers obtained by solving the following set of differential equations:

$$\begin{aligned} \mathbf{M}_\lambda \ddot{\boldsymbol{\lambda}}(t) + \mathbf{C}_\lambda \dot{\boldsymbol{\lambda}}(t) + \mathbf{K}_\lambda \boldsymbol{\lambda}(t) + \mathbf{G}_\lambda(t) \mathbf{F}(t) + \mathbf{G}_{0\lambda}(t) \mathbf{F}_0(t) &= \mathbf{P}_\lambda(t) \\ \boldsymbol{\lambda}(t_f) = \mathbf{0}, \quad \dot{\boldsymbol{\lambda}}(t_f) &= \mathbf{0} \\ \dot{\mathbf{F}}(t) = \dot{\boldsymbol{\lambda}}(t) + \mathbf{H}_\lambda(t) \mathbf{F}(t) + \mathbf{Q}_\lambda(t); \quad \mathbf{F}(t_f) &= \mathbf{0} \\ \dot{\mathbf{F}}_0(t) = \dot{\boldsymbol{\lambda}}(t) + \mathbf{H}_{0\lambda}(t) \mathbf{F}_0(t); \quad \mathbf{F}_0(t_f) &= \mathbf{0} \end{aligned} \quad (3.5)$$

where:

$$\begin{aligned} \mathbf{M}_\lambda &= \mathbf{M}; \quad \mathbf{C}_\lambda = -\mathbf{C}; \quad \mathbf{K}_\lambda = \mathbf{K}_\alpha \\ \mathbf{G}_\lambda(t) &= \left(\frac{\partial \mathbf{f}(\mathbf{v}(t), \mathbf{f}_h(t))}{\partial \mathbf{v}} \right)^T; \quad \mathbf{G}_{0\lambda}(t) = \left(\frac{\partial \mathbf{f}(\mathbf{v}(t), \mathbf{f}_{h0}(t), \mathbf{k}_0)}{\partial \mathbf{v}} \right)^T \\ \mathbf{F}(t) &= \boldsymbol{\lambda}_{ph}(t); \quad \mathbf{F}_0(t) = \boldsymbol{\lambda}_{p0}(t) \\ \mathbf{P}_\lambda(t) &= -\mathcal{D}(\mathbf{f}_h(t)) \cdot \mathcal{D}^{-1}(\mathbf{E}_{h,all}) \cdot \boldsymbol{\lambda}_{Eh}(t_f) - \int \left\{ -\frac{p}{t_f} \cdot (\mathcal{D}(\mathbf{x}(t)) \cdot \mathcal{D}^{-1}(\mathbf{d}_{all}))^{p-1} \cdot \mathcal{D}^{-1}(\mathbf{d}_{all}) \cdot \boldsymbol{\lambda}_{dmp}(t_f) \right\} dt \\ \mathbf{H}_\lambda(t) &= -\left(\frac{\partial \mathbf{f}(\mathbf{v}(t), \mathbf{f}_h(t))}{\partial \mathbf{f}_h} \right)^T; \quad \mathbf{H}_{0\lambda}(t) = -\left(\frac{\partial \mathbf{f}(\mathbf{v}(t), \mathbf{f}_{h0}(t), \mathbf{k}_0)}{\partial \mathbf{f}_{h0}} \right)^T \\ \mathbf{Q}_\lambda(t) &= -\mathcal{D}(\mathbf{v}(t)) \cdot \mathcal{D}^{-1}(\mathbf{E}_{h,all}) \cdot \boldsymbol{\lambda}_{Eh}(t_f) \\ (\boldsymbol{\lambda}_{Eh}(t_f))_n &= \frac{\partial g(\mathbf{y}(t_f))}{(\partial \mathbf{E}_h)_n} = \frac{1}{den^2} \cdot \left(den \cdot \frac{\partial num}{(\partial \mathbf{E}_h)_n} - num \cdot \frac{\partial den}{(\partial \mathbf{E}_h)_n} \right) \\ (\boldsymbol{\lambda}_{dmp}(t_f))_n &= \frac{\partial g(\mathbf{y}(t_f))}{(\partial \mathbf{d}_{m,p})_n} = \frac{1}{den^2} \cdot \left(den \cdot \frac{\partial num}{(\partial \mathbf{d}_{m,p})_n} - num \cdot \frac{\partial den}{(\partial \mathbf{d}_{m,p})_n} \right) \\ den &= \mathbf{1}^T \cdot \mathcal{D}^q \left(\frac{1}{n_{eq}} \sum_{n=1}^{n_{eq}} (\mathbf{E}_h(t_f))_n \right) \cdot \mathbf{1} + \mathbf{1}^T \cdot \mathcal{D}^q \left(\frac{1}{n_{eq}} \sum_{n=1}^{n_{eq}} \mathcal{D}^{\frac{1}{p}} (\mathbf{d}_{m,p}(t_f))_n \right) \cdot \mathbf{1} \\ num &= \mathbf{1}^T \cdot \mathcal{D}^{q+1} \left(\frac{1}{n_{eq}} \sum_{n=1}^{n_{eq}} (\mathbf{E}_h(t_f))_n \right) \cdot \mathbf{1} + \mathbf{1}^T \cdot \mathcal{D}^{q+1} \left(\frac{1}{n_{eq}} \sum_{n=1}^{n_{eq}} \mathcal{D}^{\frac{1}{p}} (\mathbf{d}_{m,p}(t_f))_n \right) \cdot \mathbf{1} \end{aligned} \quad (3.6)$$

4. EXAMPLE

A 10 story yielding steel frame excited by the SE 10 in 50 ground-motion ensemble is retrofitted using friction dampers. 2% inherent Rayleigh damping is assumed for the first and second modes. The story stiffnesses of the shear frame are $(108.566, 106.592, 102.644, 96.722, 88.826) \times 10^3 \text{ kN/m}$ for the first five stories and $78.957 \times 10^3 \text{ kN/m}$ for each of the remaining stories. A 2% secondary stiffness slope ratio for all stories was taken. The mass of each floor is 54 tons. The friction dampers are to be installed on braces added to each of the stories. As the frame is set to yield, the performance measure of choice in this example was taken as the maximum between the maximal normalized energy and inter-story drift (see Eqn. 3.3). The design variables are the stiffness of each of the added braces on which the sliding friction device is installed. For the braces, the steel's yield stress was taken as 225 MPa, while the modulus of elasticity was taken as 210,000 MPa. The relative slip displacement of each device was set to the maximum between half the allowable drift of the story where the device is located and 90% of its yield displacement (to ensure that the device slips before it yields). The slip displacement of half the allowable drift was determined by finding the slip displacement which maximizes the amount of energy dissipated by the friction device over one hysteretic cycle, given that in this cycle the drift reaches its maximal (allowable) limit. This was found by differentiating the energy with respect to the slip displacement and equating to zero. In this case, the slip displacement, $x_{y,0}$, was determined to be $0.0048m$. A reduction factor of $R=4.0$ was taken to compute the structure's yield force at each story, i.e., first the maximum elastic force obtained at each story for each ground motion considered was computed, after which the average of all ground motions was divided by R to obtain the yield force. The yield displacement of the structure was then computed based on the yield force and the elastic stiffness matrix of the structure. The allowable drift was taken as 60% of the maximal (of all stories) average drift of the bare frame. The allowable hysteretic energy was taken as 3 times the plastic energy dissipated by the bare frame in one yielding cycle. In Eqn. 3.3 p and q were taken as 10,000.

4.1. Analysis/Redesign solution

Step 1: Time-history analysis was carried out numerically for each ground motion within the chosen ensemble. The average normalized inter-story drifts of the bare frame, along with the allowable value, the average normalized hysteretic energy along with the allowable and the performance indexes can be seen in Fig. 4.1 (in white). As can be seen, the performance index exceeds the allowable value, and thus a friction damper is added at each of the peripheral locations, with initial arbitrary values (in this case a stiffness of 10,000 kN/m was added in each of the floors).

Step 2: With this initially damped frame, time history analysis was once again carried out and the inter-story drifts at all peripheral locations can be seen in Fig. 4.1 (in gray).

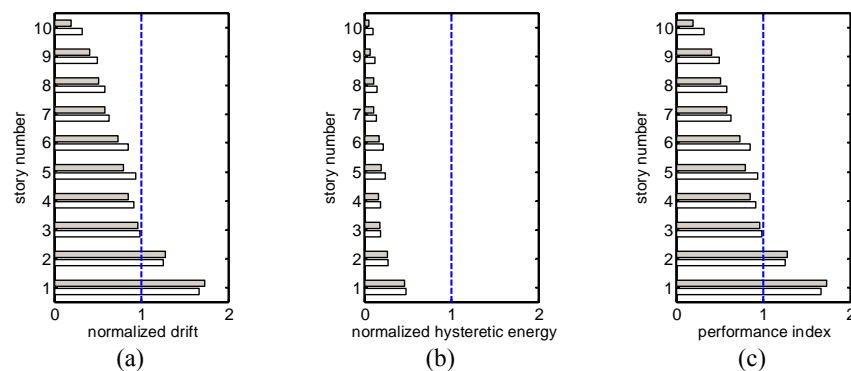


Figure 4.1. Normalized average and allowable values (dashed): (a) inter-story drifts (b) hysteretic energy and (c) performance index of the bare (white) and initially-damped (gray) structure under the SE 10 in 50 ground motion ensemble.

Step 3: As can be seen from Fig. 4.1, the initial damping distribution still leads to a performance measure which exceeds the allowable, and thus the brace stiffness is re-evaluated iteratively, using the analysis/redesign algorithm. Using this analysis/redesign procedure, at each iteration, the brace of each damper is re-evaluated using the following recurrence relation:

$$k_{0,i}^{(n+1)} = k_{0,i}^{(n)} \cdot \max \left(\left(\frac{1}{n_{eq}} \cdot \sum_{j=1}^{n_{eq}} \left(\frac{\max_i |drift(t)_i^{(n)}|}{drift_{allowable}} \right)_j \right), \left(\frac{1}{n_{eq}} \cdot \sum_{j=1}^{n_{eq}} \left(\frac{E_h(t_f)}{E_{h,allowable}} \right)_j \right) \right)^P \quad (4.1)$$

where $k_{0,i}^{(n)}$ is the added brace stiffness at location i at the n^{th} iteration, $\left(\max_i |drift(t)_i^{(n)}| \right)_j$ is the maximum absolute drift (in time) at location i obtained from earthquake j within the ensemble at the n^{th} iteration, $drift_{allowable}$ is the maximal allowable drift, n_{eq} is the number of ground motions considered and P being the convergence constant.

Step 4: Upon convergence, the brace stiffness distribution, shown in Fig. 4.2, was obtained. The final solution attained was $\mathbf{k}_0 = (4.376, 2.928, 1.888, 1.194, 0.653, 0.101) \times 10^4 \text{ kN/m}$ for the first six stories and 0.000 kN/m for each of the remaining stories. It is appropriate to mention here that the possible increase in forces due to the added stiffness of the braces is to be accommodated by the columns and foundations. Thus, there is a need to check whether these forces have been increased. In the case of this example, the final distribution of added dampers increased the average base shear by about 0.4%. With this final damping distribution, time history analysis was once again carried out for all ground motions within the chosen ensemble, and the average normalized inter-story drift, hysteretic energy and performance index obtained at each location can be seen in Fig. 4.2 (in gray), along with the values of these drifts in the bare-structure (in white) and the allowable value. As can be seen from Fig. 4.2, dampers were added only to locations for which the inter-story drifts equal the allowable, making the obtained solution a fully-stressed design. Fig. 4.3 presents the convergence of the design variables (brace stiffnesses) and the performance measure. As can be seen in Fig. 4.3, convergence is practically reached within less than 30 iterations. This was obtained for a convergence power value of $P=1$ for all iterations. The power P was found by trial and error.

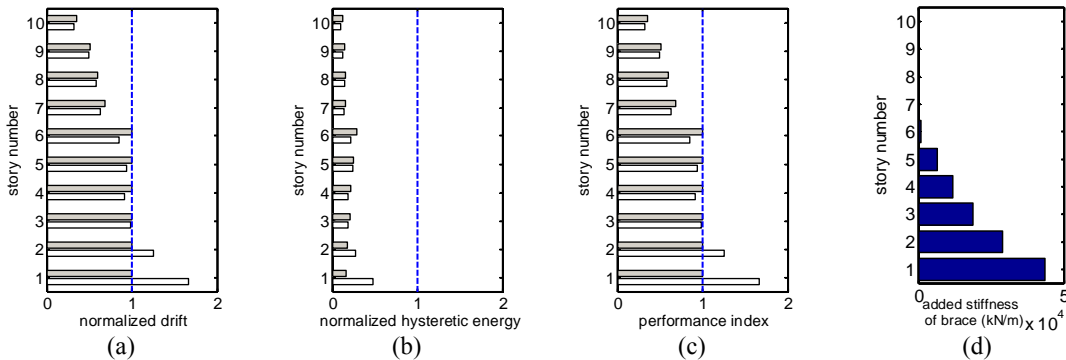


Figure 4.2. Normalized average and allowable values (dashed): (a) inter-story drifts (b) hysteretic energy (c) performance index of the bare (white) and finally-damped (gray) structure under the SE 10 in 50 ground motion ensemble and (d) final added stiffness of braces.

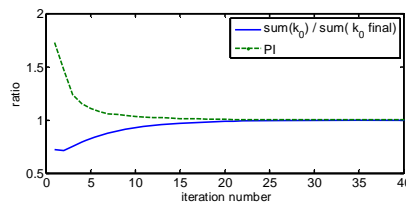


Figure 4.3. Convergence of sum of stiffness at all frames and maximal performance index.

4.2. Formal Optimization

The optimization problem was solved using the MATLAB Optimization Toolbox. The *fmincon* function was used to solve the nonlinear constrained optimization problem using the gradient-based optimization algorithm "Interior Point". The gradients of the constraint and objective function, derived in section 3.3.2, were provided for the *fmincon* function to use. The initial brace stiffness was taken as: $3.798 \times 10^5 \text{ kN/m}$ for all stories. It shall be noted that this initial distribution was selected based on a trial and error process, since not for all initial guesses the problem had converged. The normalized inter-story drifts, hysteretic energy and performance index obtained with this damping system in place can be seen in Fig. 4.4.

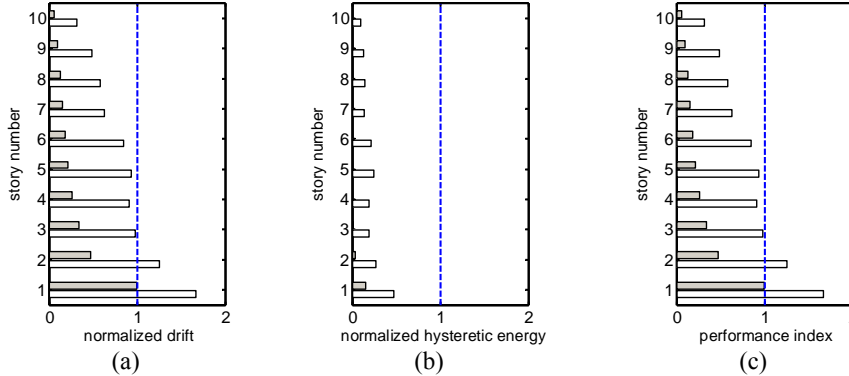


Figure 4.4. Normalized average and allowable values (dashed): (a) inter-story drifts (b) hysteretic energy and (c) performance index of the bare (white) and initially-damped (gray) structure under the SE 10 in 50 ground motion ensemble.

Using the Interior Point algorithm, the stiffness converged to the final stiffness using 962 function/gradient evaluations. The final solution attained was $\mathbf{k}_0 = (4.350, 2.906, 1.868, 1.179, 0.640, 0.0915) \times 10^4 \text{ kN/m}$ for the first six stories and 0.000 kN/m for each of the remaining stories (see Fig. 4.5). The inter-story drifts, hysteretic energy and performance indices obtained with the converged damping system in place can also be seen in Fig. 4.5. The convergence of the constraint as well as the performance index can be seen in Figs. 4.6.

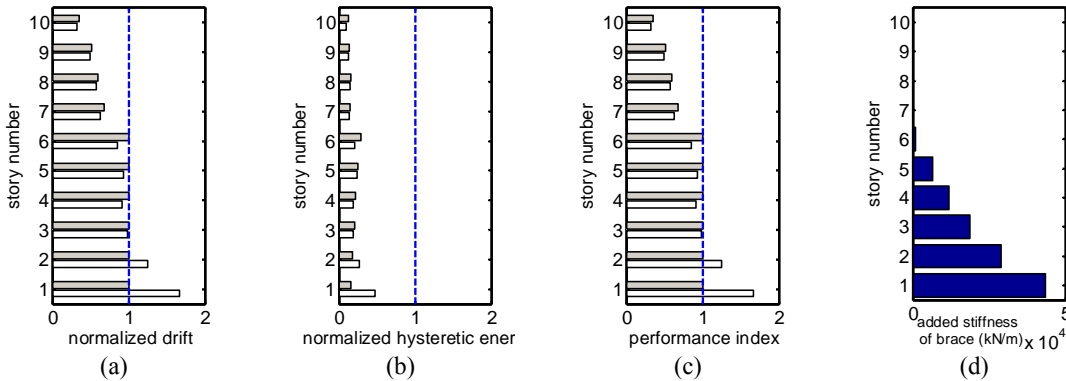


Figure 4.5. Normalized average and allowable values (dashed): (a) inter-story drifts (b) hysteretic energy (c) performance index of the bare (white) and finally-damped (gray) structure under the SE 10 in 50 ground motion ensemble and (d) final added stiffness of braces.

When comparing the solutions attained using the analysis/redesign scheme and formal optimization, it can be seen that these two are very similar. The solution obtained by the formal optimization has a very slight advantage over that obtained by the analysis/redesign scheme, as the cost value of its objective function (sum of stiffnesses) is $1.1035 \cdot 10^5$ compared to $1.1141 \cdot 10^5$ for the

analysis/redesign solution (0.95% difference, which is likely the result of different convergence criteria). Therefore, it was shown that the analysis/redesign procedure, in this case, results in an optimal solution of the optimization problem. When comparing the number of function evaluations needed for the solution to converge (the cost of computational effort, in this case), it can be seen that the analysis/redesign method is much more efficient since it only needed about 40 function evaluations to converge, while the optimization process only converged after a few hundred evaluations.

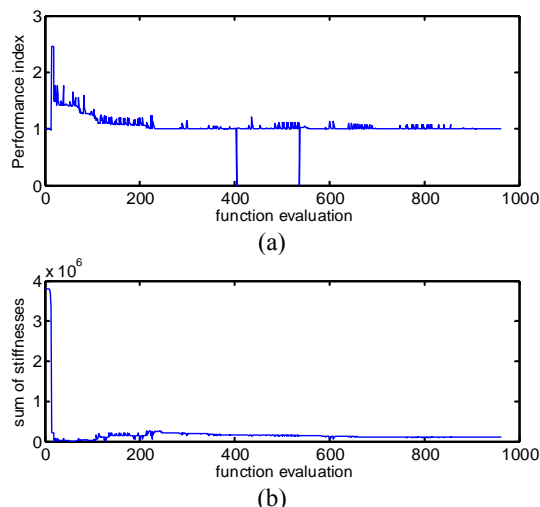


Figure 4.6. (a) Performance index (constraint) convergence and (b) Stiffness (objective function) convergence.

5. CONCLUSIONS

A performance-based methodology for optimally allocating friction/hysteretic damping devices within existing frame structures was presented. The methodology, which considers all possible dampening locations, is based on an analysis/redesign scheme, which is simple to use and does not demand many iterations to converge, making it very efficient. The methodology is general, due to its special formulation, making it applicable to any type of structure, regardless of the extent of its irregularity.

It was shown that by using friction dampers, responses can be reduced to a desired level and that the solution attained is a fully-stressed design. To validate the optimality of the solution obtained by the analysis/redesign procedure, the optimization problem was also solved using formal optimization tools. This required the evaluation of the gradients, which were derived for both the objective function and the constraints, using the calculus of variations. For the case presented, it was shown that the optimal solution attained using the formal optimization is very close to the solution targeted by the analysis/redesign procedure, which may, therefore, be regarded as an optimal solution. This reinforces previous results which were referenced and discussed herein. Moreover, it was shown that the analysis/redesign method is a much faster converging process, which requires much less computational effort. This is the case since even if the number of needed iterations is similar, the analysis/redesign method only requires analyses computations, while the formal optimization requires, in addition, Lagrange multipliers and gradient computations. Therefore, the analysis/redesign method is much more practical for use.

REFERENCES

- Apostolakis, G. and Dargush, G.F. (2010). Optimal Seismic Design of Moment-Resisting Steel Frames with Hysteretic Passive Devices. *Earthquake Engineering and Structural Dynamics*, **39**, 355-376.
- Benavent-Climent, A. (2011). An Energy-Based Method for Seismic Retrofit of Existing Frames using Hysteretic Dampers. *Soil Dynamics and Earthquake Engineering*, **31**, 1385-1396.
- Cherry, S. and Filiatrault, A. (1993). Seismic Response Control of Buildings Using Friction Dampers. *Earthquake Spectra*, **9:3**, 447-466.
- Choi, H. and Kim, J. (2006). Energy-Based Seismic Design of Buckling-Restrained Braced Frames Using

- Hysteretic Energy Spectrum. *Engineering Structures*. **28**, 304-311.
- Cilley, F.H. (1900). The Exact Design of Statically Indeterminate Frameworks, an Exposition of its Possibility but Futility. Transactions, ASCE. **43**, 353-407.
- Daniel, Y., Nsier, I., Lavan, L. and Levy, R. (2010). Optimal Allocation and Sizing of Friction Dampers for Seismic Control. *Proceedings of the 14th European Conference on Earthquake Engineering, Ohrid, Macedonia*. Paper No. 1055.
- Dargush, G.F. and Sant R.S. (2005). Evolutionary Aseismic Design and Retrofit of Structures with Passive Energy Dissipation. *Earthquake Engineering and Structural Dynamics*. **34**, 1601-1626.
- Farhat, F., Nakamura, S. and Takahashi, K. (2009). Application of Genetic Algorithm to Optimization of Buckling Restrained Braces for Seismic Upgrading of Existing Structures. *Computers and Structures*. **87**, 110-119.
- Inoue, K. and Kuwahara, S. (1998). Optimum Strength Ratio of Hysteretic Damper. *Earthquake Engineering and Structural Dynamic*. **27**, 577-588.
- Lavan, O. (2006). Seismic Behavior and Control of Irregular Structures: an Energy Approach. Ph.D. dissertation, Technion – Israel Institute of Technology, Haifa, Israel.
- Lavan, O. and Dargush, G.F. (2009). Multi-Objective Evolutionary Seismic Design Passive Energy Dissipation Systems. *Journal of Earthquake Engineering*. **13:6**, 758-790.
- Lee, S.H., Park, J.H., Lee, S.K. and Min K.W. (2008). Allocation and Slip Load of Friction Dampers for a Seismically Excited Building Structure Based on Storey Shear Force Distribution. *Engineering Structures*. **30**, 930-940.
- Levy, R. (1985). On the Optimal Design of Trusses under One Loading Condition. *Quarterly of Applied Mathematics*. **43:2**, 129-134.
- Levy, R. and Lavan, O. (2006). Fully Stressed Design of Passive Controllers in Framed Structures for Seismic Loadings. *Journal of Structural and Multidisciplinary Optimization*. **32**, 485-498.
- Levy, R., Lavan, O. and Rutenberg, A. (2005). Seismic Design of Friction-Damped Braced Frames Based on Historical Records. *Earthquake Spectra*. **21:3**, 761-778.
- Levy, R., Marianchik, E., Rutenberg A. and Segal, F. (2001). A Simple Approach to the Seismic Design of Friction Damped Braced Medium-Rise Frames. *Engineering Structures*. **23**, 250-259.
- Liu, W., Tong, M. and Lee, G.C. (2005). Optimization Methodology for Damper Configuration Based on Building Performance Indices. *Journal of Structural Engineering*. **131:11**, 1746-1756.
- Lopez Garcia, D. (2001). A Simple Method for the Design of Optimal Damper Configuration in MDOF Structures. *Earthquake Spectra*. **17:3**, 387-398.
- Moreschi, L.M. and Singh, M.P. (2003). Design of Yielding Metallic and Friction Dampers for Optimal Seismic Performance. *Earthquake Engineering and Structural Dynamics*. **32**, 1291-1311.
- Ok, S.Y., Song, J. and Park, K.S. (2008). Optimal Design of Hysteretic Dampers Connecting Adjacent Structures Using Multi-objective Genetic Algorithm and Stochastic Linearization Method. *Engineering Structures*. **30**, 1240-1249.
- Ozdemir, H. (1976). Nonlinear Transient Dynamic Analysis of Yielding Structures. Ph.D. dissertation, University of California, Berkeley, USA.
- Sivalsevan, M.V. and Reinhorn, A.M. (2000). Hysteretic Models for Deteriorating Inelastic Structures. *Journal of Engineering Mechanics*. **126:6**, 633-640.
- Soong, T.T. and Dargush, G.F. (1997). *Passive Energy Dissipation Systems in Structural Engineering*, John Wiley & Sons Ltd., Chichester.
- Symans, M.D., Charney F.A., Whittaker, A.S., Constantinou, M.C., Kircher, C.A., Johnson, M.W. and McNamara, R.J. (2008). Energy Dissipation Systems for Seismic Applications: Current Practice and Recent Development. *Journal of Structural Engineering*. **134:1**, 3-11.
- Wongprasert, N. and Symans, M.D. (2004). Application of a Genetic Algorithm for Optimal Damper Distribution within the Nonlinear Seismic Benchmark Building. *Journal of Engineering Mechanics*. **130:4**, 401-406.
- Xu, Y.L. and Teng, J. (2002). Optimum Design of Active/Passive Control Devices for Tall Buildings under Earthquake Excitation. *The Structural Design of Tall Buildings*. **11**, 109-127.
- Yang, J. N., Lin, S., Kim, J-H. and Agrawal, A. K. (2002). Optimal Design of Passive Energy Dissipation Systems Based on H_{∞} and H_2 Performances. *Earthquake Engineering and Structural Dynamics*, **31**, 921-936.